A tunable and switchable single-longitudinal-mode dual-wavelength fiber laser with a simple linear cavity

Xiaoying He,[1] Xia Fang,[1] Changrui Liao, [1] D. N. Wang, [1,*] and Junqiang Sun[2]

[1]*Department of Electrical Engineering, The Hong Kong Polytechnic University, Hung Hom, Kowloon, Hong Kong*

[2]*Wuhan national Laboratory for Optoelectronics, Huazhong University of Science and Technology, Wuhan, 430074, P. R. China*

[*]*eednwang@polyu.edu.hk*

Abstract: A simple linear cavity erbium-doped fiber laser based on a Fabry-Perot filter which consists of a pair of fiber Bragg gratings is proposed for tunable and switchable single-longitudinal-mode dual-wavelength operation. The single-longitudinal-mode is obtained by the saturable absorption of an unpumed erbium-doped fiber together with a narrow-band fiber Bragg grating. Under the high pump power (>166mW) condition, the stable dual-wavelength oscillation with uniform amplitude can be realized by carefully adjusting the polarization controller in the cavity. Wavelength selection and switching are achieved by tuning the narrow-band fiber Bragg grating in the system. The spacing of the dual-wavelength can be selected at 0.20nm (~ 25.62GHz), 0.22nm (~ 28.19GHz) and 0.54nm (~ 69.19GHz).

©2009 Optical Society of America

OCIS codes: (000.0000) General; (000.2700) General science.

References and links

1. N. J. C. Libatique, and R. K. Jain, "Precisely and rapidly wavelength-switchable narrow-linewidth 1.5μm laser source for wavelength division multiplexing applications," IEEE Photon. Technol. Lett. **11**(12), 1584–1586 (1999).
2. Z. Chen, S. Ma, and N. K. Dutta, "Stable dual wavelength mode-locked Erbium-doped fiber ring laser," in Frontiers in Optics, OSA Technical Digest, paper FTuG6
3. P.-C. Peng, H.-Y. Tseng, and S. Chi, "A tunable dual-wavelength erbium-doped fiber ring laser using a self-seeded fabrycprot laser diode," IEEE Photon. Technol. Lett. **15**(5), 661–663 (2003).
4. J. Liu, J. P. Yao, J. Yao, and T. H. Yeap, "single-longitudinal-mode multiwavelength fiber ring laser," IEEE Photon. Technol. Lett. **16**(4), 1020–1022 (2004).
5. S. Pan, and J. P. Yao, "A wavelength-switchable single-longitudinal-mode dual-wavelength erbium-doped fiber laser for switchable microwave generation," Opt. Express **17**(7), 5414–5419 (2009).
6. Y. Yao, X. Chen, and S. Xie, "Dual-wavelength erbium-doped fiber laser with a simple linear cavity and its application in microwave generation," IEEE Photon. Technol. Lett. **18**(1), 187–189 (2006).
7. G. Chen, D. Huang, X. Zhang, and H. Cao, "Photonic generation of a microwave signal by incorporating a delay interferometer and a saturable absorber," Opt. Lett. **33**(6), 554–556 (2008).
8. S. L. Pan, X. F. Zhao, and C. Y. Lou, "Switchable single-longitudinal-mode dual-wavelength erbium-doped fiber ring laser incorporating a semiconductor optical amplifier," Opt. Lett. **33**(8), 764–766 (2008).
9. C. C. Lee, Y. K. Chen, and S. K. Liaw, "Single-longitudinal-mode fiber laser with a passive multiple-ring cavity and its application for video transmission," Opt. Lett. **23**(5), 358–360 (1998).
10. M. Matsuura, and N. Kishi, "Frequency control characteristics of a single-frequency fiber laser with an external light injection," IEEE J. Sel. Top. Quantum Electron. **7**(1), 55–58 (2001).
11. Y. Cheng, J. T. Kringlebotn, W. H. Loh, R. I. Laming, and D. N. Payne, "Stable single-frequency traveling-wave fiber loop laser with integral saturable-absorber-based tracking narrow-band filter," Opt. Lett. **20**(8), 875–877 (1995).
12. H. Y. Ryu, W. K. Lee, H. S. Moon, S. K. Kim, H. S. Suh, and D. Lee, "Stable single-frequency fiber ring laser for 25-GHz ITU-T utilizing saturable absorber filter," IEEE Photon. Technol. Lett. **17**(9), 1824–1826 (2005).
13. K. Zhang, and J. U. Kang, "C-band wavelength-swept single-longitudinalmode erbium-doped fiber ring laser," Opt. Express **16**(18), 14173–14179 (2008).

#117766 - $15.00 USD Received 25 Sep 2009; revised 6 Nov 2009; accepted 8 Nov 2009; published 12 Nov 2009

14. X. P. Cheng, P. Shum, C. H. Tse, J. L. Zhou, M. Tang, W. C. Tan, R. F. Wu, and J. Zhang, R, F. Wu, and J. Zhang, "Single-longitudinal-mode erbium-doped fiber ring laser based on high finesse fiber bragg grating Fabry-Perot Etalon," IEEE Photon. Technol. Lett. **20**(12), 976–978 (2008).
15. J. Sun, X. Yuan, X. Zhang, and D. Huang, "Single-longitudinal-mode fiber ring laser using fiber grating-based Fabry-Perot filters and variable saturable absorbers," Opt. Commun. **267**(1), 177–181 (2006).
16. K. Murasawa, and T. Hidaka, "Extension of dual-wavelength region in semiconductor laser with distributed Bragg Reflector," Jpn. J. Appl. Phys. **48**(1), 010208–1 (2009).
17. Y. Li, C. R. Liao, D. N. Wang, T. Sun, and K. T. V. Grattan, "Study of spectral and annealing properties of fiber Bragg gratings written in H_2-free and H_2- loaded fibers by use of femtosecond laser pulses," Opt. Express **16**(26), 21239–21247 (2008).
18. T. Erdogan, "Fiber grating spectra," J. Lightwave Technol. **15**(8), 1277–1294 (1997).

1. Introduction

Dual-wavelength fiber laser with narrow line-width single-longitudinal-mode (SLM) operation and uniform amplitude output has attracted a lot of research interests because of its potential applications in optical communications, optical instrument testing and optical fiber sensors [1–3]. Especially, a wavelength tunable or switchable SLM dual-wavelength fiber laser is considered to be a desirable candidate for frequency-tunable, high-power, and low phase noise microwave or millimeter-wave generation [4–7], as microwave generation in this way does not require a high-quality frequency-tunable microwave reference source and thus reducing the system cost and complexity. However, to ensure a stable operation of the erbium-doped fiber (EDF) laser, two major issues need to be carefully addressed. Firstly, the strong homogeneous line broadening and cross-gain saturation in the EDF would lead to an unstable SLM dual-wavelength oscillation. A number of approaches have been proposed to overcome this difficulty such as the use of a hybrid gain medium [8], a passive multiple ring cavity [8], an external light injection [9], an unpumped EDF as a saturable absorber (SA) based narrow bandwidth filter [5,10–12], etc. Secondly, an ultranarrow mode selecting mechanism should be utilized to eliminate the multi-longitudinal-mode oscillation and mode competition, caused by the long cavity length and hence the narrow longitudinal mode spacing. Such an ultranarrow bandpass filter can be obtained by using a phase shifted fiber Bragg grating (FBG) [6], an SA based Sagnac loop [13], or an FBG-based Fabry-Perot (F-P) filter [14,15]. Although the FBG based F-P filter has been utilized in the ring cavity of fiber laser to realize the SLM operation [14,15], no single to dual wavelength switching can be achieved. However, either no SA element is used for stabilizing the output power [14], or a segment of gain fiber and a pump diode are employed to function as the SA element [15]. Despite the capability of supporting a dual-wavelength oscillation by some semiconductor lasers, it is still not convenient to achieve a reliable dual-wavelength oscillation because of the strong competition between the two wavelengths [16].

In this paper, we propose a novel linear-cavity EDF laser based on an FBG-based F-P filter, which generates a wavelength tunable and switchable SLM dual-wavelength lasing. The operating wavelengths and their spacing can be selected by use of an FBG-based F-P filter together with a narrow-band FBG in the laser cavity. An umpumed EDF is used as an SA which, together with a narrow-band FBG, helps in achieving stable SLM operation. When compared with the ring cavity laser with an FBG-based F-P filter and the same length of SA with FBG, our system exhibits the advantage of providing double optical gain in the EDF. Thus, our system has high potential in frequency-tunable microwave generation.

2. Operation principle and experimental setup

Figure 1 shows the configuration of the proposed tunable and switchable dual-wavelength SLM EDF laser. The EDF (Highwave-tech EDF-741) with a length of 12 meters is used as the gain medium, pumped with a 980nm laser diode (LD) through a 980nm/1550nm wavelength division multiplexing (WDM) coupler (50:50). The absorption coefficient of the EDF at 1530nm is ~ 6-8 dB/m. The laser output is monitored by an optical spectrum analyzer (ANDO AQ6319) with 0.01nm resolution. By adjusting the narrow-band FBG, the lasing wavelengths can be tuned and switched. The experiment is carried out at room temperature and the results obtained show good stability.

#117766 - $15.00 USD Received 25 Sep 2009; revised 6 Nov 2009; accepted 8 Nov 2009; published 12 Nov 2009
(C) 2009 OSA

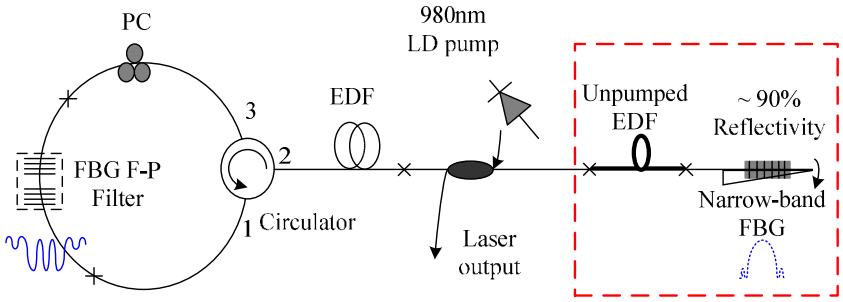

Fig.1. Schematic diagram of the proposed tunable and switchable dual-wavelength Erbium-doped fiber laser with a simple linear cavity

2.1 narrow-band FBG and FBG-based F-P filter

The narrow-band FBG shown in Fig. 1 has a reflection peak at 1569.81nm, with peak reflectivity of over 90% and a 3-dB band width of 0.71nm. Such an FBG is used to form a standing wave in the SA, to reflect the desirable wavelengths, and it is type-II grating written in H_2-free SMF-28 fiber by use of 800nm/120fs femto-second laser pulses and a phase mask (Ibsen Photonics). The laser pulse energy is 400-480μJ, with 1/e Gaussian beam radius of 3mm, and exposure time of ~45 min. This type of FBG exhibits high temperature stability and good spectral quality [17]. The reflection spectrum of this narrow-band FBG is shown in Fig. 2.

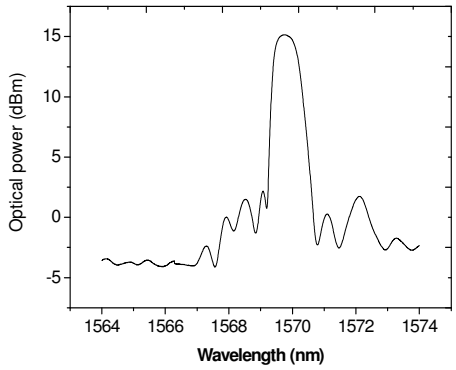

Fig. 2. Reflectivity spectrum of the narrow-band FBG

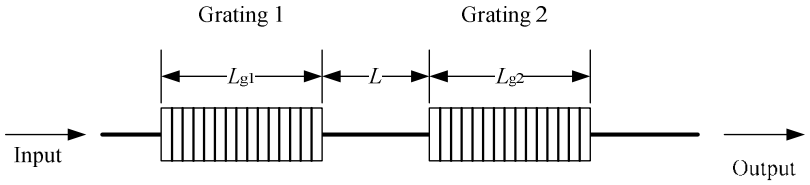

Fig. 3. Scheme of the fiber Bragg grating based Fabry-Perot filter

As shown in Fig. 3, the FBG-based F-P filter used in the configuration is composed of a pair of FBGs with a short length of 3mm and a position separation of 1.7mm, fabricated also by use of femtosecond laser pulses through a phase mask (Ibsen Photonics). The two FBGs with the same length of 3mm are fabricated under the same condition of ~25 min exposure time. Such an F-P filter has two transmission peaks represented by channel C2 and C3 respectively, and several side-lobes at the wavelengths indicated by C0, C1 and C4,

#117766 - $15.00 USD Received 25 Sep 2009; revised 6 Nov 2009; accepted 8 Nov 2009; published 12 Nov 2009
(C) 2009 OSA

respectively, as shown in Fig. 4(a). The line-width of the two transmission peaks is less than 0.01nm, which is beyond the resolution limit of the OSA used. The transfer matrixes of the two FBGs are expressed as [18]:

$$F_1 = \begin{bmatrix} \cosh\left(\gamma L_{g1(2)}\right) - j\frac{\sigma}{\gamma}\sinh\left(\gamma L_{g1(2)}\right) & -j\frac{\kappa}{\gamma}\sinh\left(\gamma L_{g1(2)}\right) \\ j\frac{\kappa}{\gamma}\sinh\left(\gamma L_{g1(2)}\right) & \cosh\left(\gamma L_g\right) + j\frac{\sigma}{\gamma}\sinh\left(\gamma L_{g1(2)}\right) \end{bmatrix} \quad (1)$$

where κ is the couple coefficient and $\gamma = \sqrt{\kappa^2 - \sigma^2}$. $L_{g1(2)}$ is the length of grating 1 and grating 2. The transfer matrix of the position separation between two FBGs can be expressed as [18]:

$$F_2 = \begin{bmatrix} e^{j\beta L} & 0 \\ 0 & e^{-j\beta L} \end{bmatrix} \quad (2)$$

where, L is the position separation of the two FBGs. Using the transfer matrix method, the transmission of the FBG-based F-P filter can be expressed as:

$$T = \frac{2j\frac{\kappa}{\gamma}\sinh\left(\gamma L_g\right)\left[\cosh\left(\gamma L_g\right)\cos\left(\beta L\right) - \frac{\sigma}{\gamma}\sinh\left(\gamma L_g\right)\sin\left(\beta L\right)\right]}{\left[\cosh\left(\gamma L_g\right) - j\frac{\sigma}{\gamma}\sinh\left(\gamma L_g\right)\right]^2 e^{-j\beta L} + \frac{\kappa^2}{\gamma^2}\sinh^2\left(\gamma L_g\right)e^{j\beta L}} \quad (3)$$

By use of Eq.(3), the transmission spectrum of the FBG-based F-P filter can be simulated and its result is shown in Fig.4(b), where the index change value is 1.6×10^{-4}. It can be seen from Fig.4 that, the measured spectrum shows a good agreement with the calculated one. The free spectral range (FSR) is readily derived as:

$$FSR = \frac{c}{2n_{eff}L + c\left(\tau_1(\lambda) + \tau_2(\lambda)\right)} \quad (4)$$

where c is the velocity of the light in vacuum. $\tau_1(\lambda)$ and $\tau_2(\lambda)$ are the time delays of the two grating, defined as:

$$\tau_{1(2)}(\lambda) = -\frac{\lambda^2}{2\pi c}\frac{d\varphi}{d\lambda} \quad (5)$$

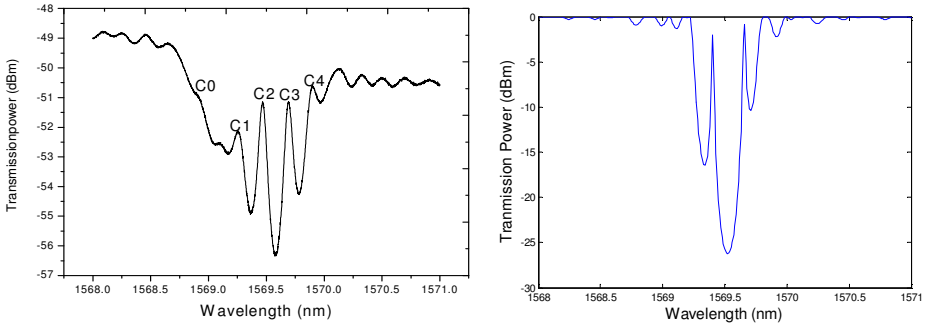

Fig. 4. Transmission spectrum of the FBG F-P filter, two FBG length of 3mm; the interval between two FBG of 1.7mm (a) measured spectrum (OSA resolution: 0.01nm); (b) calculated spectrum by transfer matrix method

#117766 - $15.00 USD Received 25 Sep 2009; revised 6 Nov 2009; accepted 8 Nov 2009; published 12 Nov 2009
(C) 2009 OSA

The FSR of the FBG-based F-P filter is mainly determined by the length of the position separation L and varies with the resonance wavelengths in the FBG.

2.2 Operation principle of saturable absorbers

In the setup, a 2-m long unpumped EDF is used as an SA. Because the absorption coefficient of an EDF is inversely proportional to the intensity of the optical light in the fiber laser, when a standing wave is formed, the spatial optical power would distribute periodically along the EDF. Therefore, an absorption coefficient with periodic variation along the SA would be created, which would results in a periodic refractive index change based on the well-known Karamer-Kronig relation, a weakly coupled longer FBG is thus generated [13]. Such a weakly coupled and narrowband FBG would form a self-tracking FBG, which can stabilize single or dual mode output. In our system, considering two waves counter-propagating in the linear arm, the whole cavity length is ~30.5m, and the laser cavity FSR is close to 6.6MHz. However, considering the unpumped EDF length of $L_e \approx 2$m, and the effective refraction index of the EDF $n_{eff} \approx 1.48$, the 3-dB bandwidth of the self-tracking FBG should be less than 6.6MHz (FSR of the laser cavity), indicating that the SLM condition would be well satisfied. In other words, simultaneous SLM lasing at dual-wavelength is ensured.

Thus, the unpumped EDF of two meter length in the linear cavity is utilized in our system as a SA which, together with a narrow-band FBG, can enhance the SLM performance and balance the optical powers of the lasing wavelengths.

3. Experimental results and discussion

The tunable and switchable dual-wavelength emission for the fiber laser is shown in Fig. 5. When the reflection peak of the narrow-band FBG overlaps with one transmission peak (C3) and the adjacent sidelobe (C4) as shown in Fig. 5(a), a dual-wavelength emission can be obtained at 1569.61nm and 1569.81nm with a wavelength spacing of 0.20nm (~ 25.62GHz). If the reflection peak of the narrow-band FBG is shifted to overlap only with C3, a single wavelength emission at 1569.60 nm can be observed as shown in Fig. 5(b). When the reflection peak of the narrow-band FBG overlap with two transmission peaks (C2 and C3) of the F-P filter, another dual-wavelength operation can be established at 1569.38nm and 1569.60nm with the wavelength spacing of 0.22nm (~ 28.19 GHz), as shown in Fig.5(c). If the narrow-band FBG peak overlaps with only C2, a single wavelength emission at 1569.38 nm appears as shown in Fig. 5(d). Finally, by shifting the reflection peak of the narrow-band FBG to overlap with the channels C0, C1, and C2, dual-wavelength operation builds up again.

Since the channel of C1 has a relatively large loss in this linear cavity than that of other channels C0 and C2, the wavelength in C1 is suppressed by the mode competitions in pumped EDF. Thus, a dual-wavelength emission is obtained in the C1 and C2 of the FBG-based F-P filter at 1568.84nm and 1569.38nm, corresponding to the wavelength spacing of 0.54nm (~ 67.19 GHz). By tuning the reflection peak of the narrow-band FBG, laser wavelength switching and dual-wavelength operation can be achieved and, the spacing of the dual-wavelength can be selected at 0.20nm (~ 25.62GHz), 0.22nm (~ 28.19GHz) and 0.54nm (~ 67.19 GHz).

The wavelengths outside of the reflection band of the FBG would pass through the FBG-based F-P filter, and then travel back into the linear cavity gain medium, and it could also transmit through the narrow-band FBG at the other end of the linear cavity and then leaks out. Thus, the wavelengths outside of the reflection band of the FBG cannot oscillate in the fiber laser system.

#117766 - $15.00 USD Received 25 Sep 2009; revised 6 Nov 2009; accepted 8 Nov 2009; published 12 Nov 2009
(C) 2009 OSA

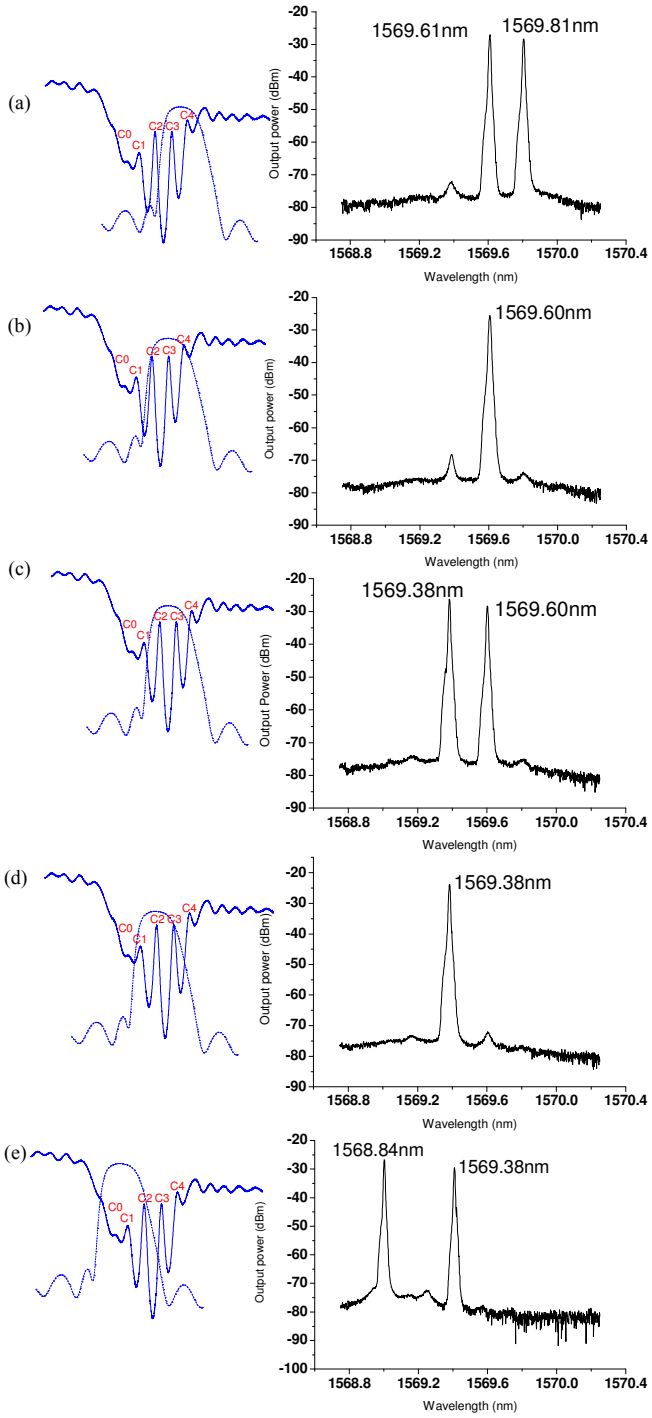

Fig. 5. Operation principle about the fiber laser with the tunable and switchable dual-wavelength emitting with pump power of 166mW; (a) dual-wavelength emitting at 1569.61 and 1569.81nm; (b) single wavelength emitting at 1569.60nm; (c) dual-wavelength emitting at 1569.38 and 1569.60nm; (d) single wavelength emitting at 1569.38nm; (e) dual-wavelength emitting at 1568.84 and 1569.38nm

#117766 - $15.00 USD Received 25 Sep 2009; revised 6 Nov 2009; accepted 8 Nov 2009; published 12 Nov 2009
(C) 2009 OSA

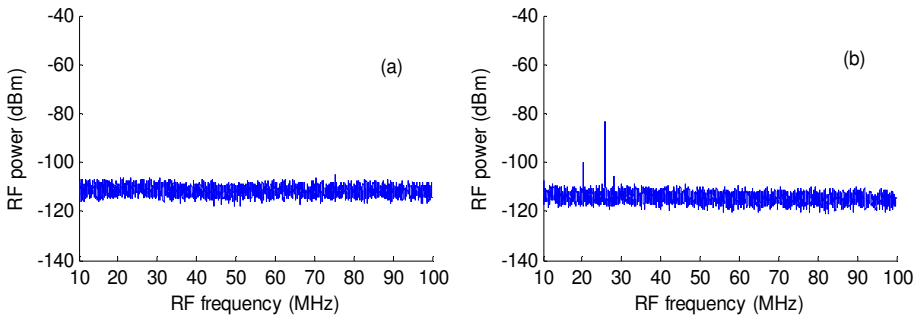

Fig. 6. Electrical spectrum of the beating signal observed at the output of the photodetector (a) SLM operation (b) mode competition and hopping

To verify the SLM operation condition of our system, we have measured the beating RF spectrum by injecting the laser output into a high speed photodetector (< 25GHz) and a 3 GHz RF spectrum analyzer [13,15], as shown in Fig. 6. There is no beating signal generation between the main lasing mode and the side modes in Fig. 6(a), as expected. Fig. 6(b) presents mode competition and hopping in the fiber laser. Thus, the SLM operation of our laser system is ensured.

In order to investigate the laser output stability and amplitude-equilibrium, the output power of the dual-wavelength at 1569.38 and 1569.60nm have been measured for different pump power levels.

Under the pump power of 166mW at 980nm, the measured output spectrum at dual-wavelengths of 1569.38 and 1569.60nm for 10 minutes is shown in Fig. 7, in which the stability time is longer than that reported in the literature [6]. Thus, the microwave local oscillator frequency can be generated in this fiber laser. The output power is ~ -25dB and the signal-to-noise ratio is ~50dB. In the situation of room temperature, the maximum power fluctuation at dual-wavelength is ~2dB, and the wavelength fluctuation is beyond the resolution limit of our OSA, as shown in Fig. 7(b). We believe that a more stable dual-wavelength lasing can be achieved if the stability of the pump LD is improved.

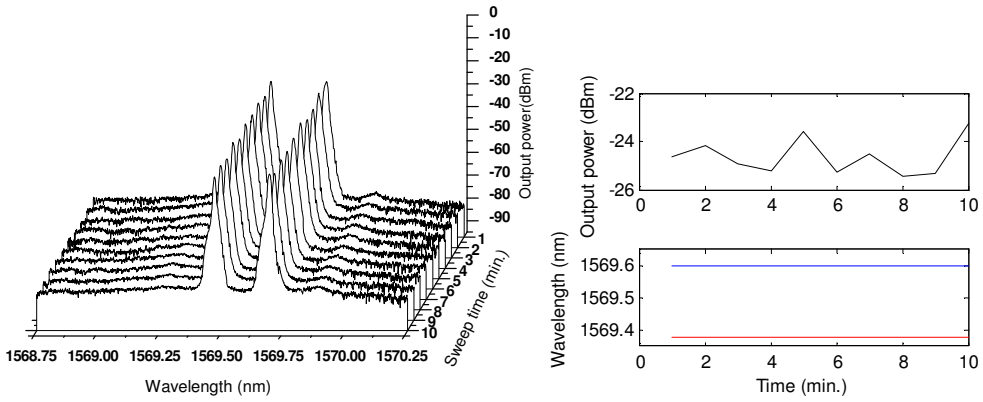

(a) (b)

Fig. 7. (a). Measured output spectrum at fixed wavelengths of 1569.38 and 1569.60nm every 1 minutes for 10 minutes, pump power of 166mW; (b). Fluctuation of output power and wavelength during 10 minutes

Under the pump power of 133mW, by carefully adjusting the state of the PC, single-wavelength or dual-wavelength operations can be obtained, as shown in Fig. 8. Fig. 9 demonstrates the dual-wavelength operations with the pump power of 166mW, where the switching from dual-wavelength to single-wavelength lasing cannot be reached by adjusting

#117766 - $15.00 USD Received 25 Sep 2009; revised 6 Nov 2009; accepted 8 Nov 2009; published 12 Nov 2009
(C) 2009 OSA

the state of the PC. That is because, under the low pump power, the unpumed EDF in the linear cavity does not reach the saturated absorption condition, and when the polarization state in the fiber cavity is adjusted, one of emitting wavelengths can be easily suppressed. When the pump power becomes high, the unpumped EDF reaches its saturated absorption condition, and the function of the PC is to balance the gain and loss corresponding to the polarization state, hence, a uniform amplitude dual-wavelength laser operation can be obtained.

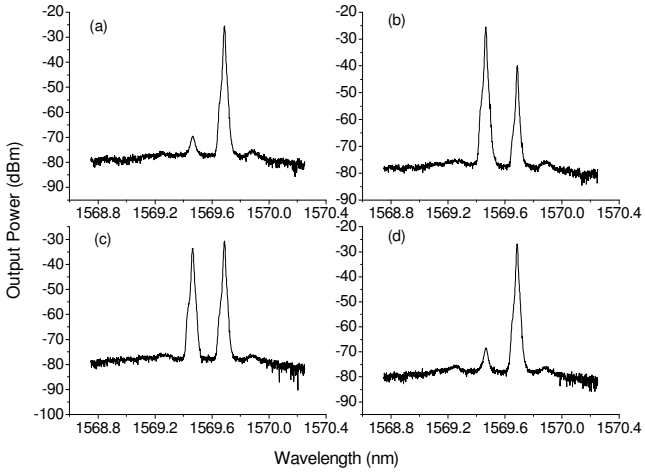

Fig. 8. Wavelength switching of the fiber laser by adjusting the PC, with low pump power of 133mW

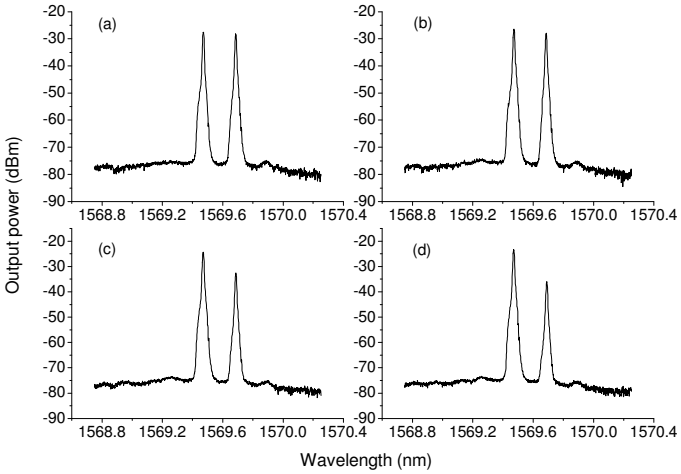

Fig. 9. Dual-wavelength emission of the fiber laser by adjusting the PC, with high pump power of 166mW

By changing the pump power from 133mW to 188.4mW, the output power variation of the dual-wavelength lasing at 1569.38 and 1569.60nm is shown in Fig. 10. When the pump power is lower than 155mW, as shown in the inset (two dimensional graph showing output wavelength power vs. pump power) of Fig. 10, a large output power variation can be observed, which indicates a large output power competition may exist in these two emitting wavelengths. Thus, the uniform amplitude dual-wavelength laser operation cannot be maintained. When the pump power is larger than 155mW, the SA plays a significant role, and an uniform amplitude and stable dual-wavelength operation can be maintained.

#117766 - $15.00 USD Received 25 Sep 2009; revised 6 Nov 2009; accepted 8 Nov 2009; published 12 Nov 2009
(C) 2009 OSA

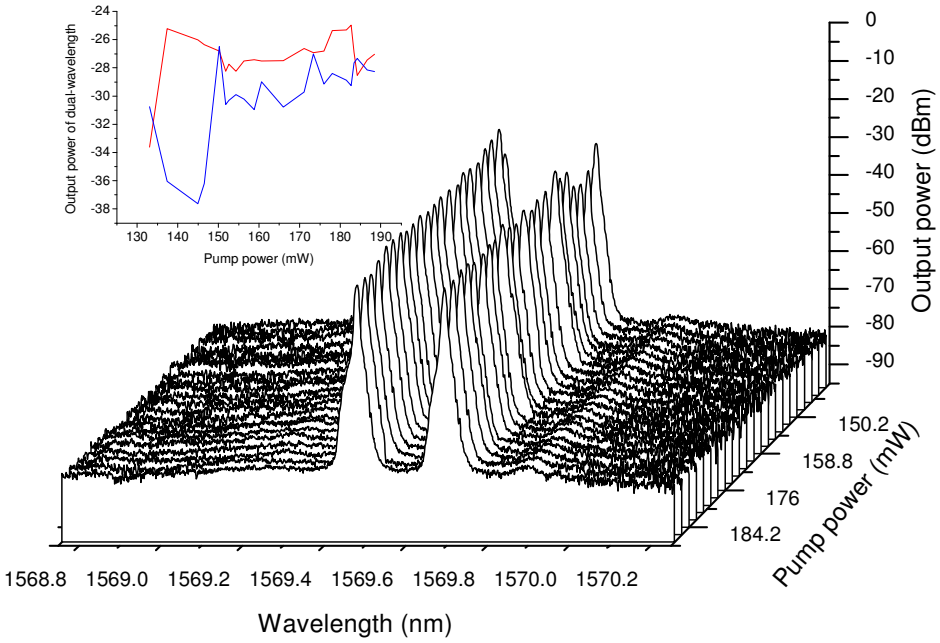

Fig. 10. Measured output spectrum at fixed wavelengths of 1569.38 and 1569.60nm with changing the pump power from 133mW to 188.4mW; Inset: red line corresponds to the wavelength of 1569.38 nm and blue line corresponds to the wavelength of 1569.60 nm

4. Conclusion

A novel EDF laser with tunable and switchable dual-wavelength SLM operation is proposed and experimentally demonstrated. The main components of the system include an F-P filter based on a pair of FBGs, an umpumped EDF and a narrow-band FBG. The unpumped EDF together with the narrow-band FBG are used to ensure the SLM operation and balance the lasing wavelength power. The lasing wavelength and their spacing are selected by use of the F-P filter and the narrow-band FBG. The single-wavelength or dual-wavelength operation can be switched by controlling the overlap of the narrow-band FBG reflection peak and the transmission peaks of the F-P filter. When the pump power is lowered to 133mW, the laser can operate in either single-wavelength or dual-wavelength by adjusting the PC. Under the high pump power (>166mW) condition, the uniform amplitude dual-wavelength lasing can be obtained by carefully adjusting the PC. The system has high potential in generation of frequency-tunable microwave signal for radio-over-fiber systems and wireless networks.

Acknowledgment

This work is supported by the Hong Kong Polytechnic University research grants G-YX2N and A-PJ22.

#117766 - $15.00 USD Received 25 Sep 2009; revised 6 Nov 2009; accepted 8 Nov 2009; published 12 Nov 2009
(C) 2009 OSA